Limnology and Oceanography

FLUIDS & ENVIRONMENTS

ORIGINAL ARTICLE

The impact of fine-scale turbulence on phytoplankton community structure

Andrew D. Barton,[1,2] Ben A. Ward,[3] Richard G. Williams,[4] and Michael J. Follows[1]

Abstract

We examined the effect of fine-scale fluid turbulence on phytoplankton community structure in an idealized, size-structured community model. It has been shown that turbulence can enhance nutrient transport toward a cell, particularly for larger cells in highly turbulent conditions. Our model suggests that under weak grazing pressure the effect of this mechanism on relative phytoplankton fitness and community structure is negligible. Under these conditions, the high nutrient affinity of small cells dominates relative fitness and allows them to outcompete larger cells. In contrast, when grazing pressure is strong, the turbulent enhancement of nutrient uptake and fitness for larger cells can become ecologically significant. Here, increasing turbulence broadens the size range of coexisting phytoplankton and increases the size of the dominant cell type at equilibrium. We also estimate and map open ocean turbulent dissipation rates as a function of climatological surface wind stresses. The turbulent enhancement of nutrient uptake is most likely to be ecologically significant in regions with low nutrient levels, strong grazing pressure, and relatively high turbulence, such as in windier portions of the subtropical gyre or post-bloom conditions at higher latitudes. In these regions, turbulence may help sustain larger cell populations through otherwise unfavorable environmental conditions.

Keywords: cell size, diffusion, zooplankton grazing, microbial, nutrient uptake

[1]Department of Earth, Atmospheric, and Planetary Sciences, Massachusetts Institute of Technology, Cambridge, Massachusetts 02139, USA

[2]Division of Earth and Ocean Sciences, Nicholas School of the Environment, Duke University, Durham, North Carolina 27708, USA

[3]Centre d'Enseignement et de Recherches sur l'Environnement et la Société, Environmental Research and Teaching Institute, École Normale Supérieure, F-75230 Paris cedex 05, France

[4]School of Environmental Sciences, University of Liverpool, Liverpool L69 3GP, United Kingdom

Correspondence to Andrew D. Barton, andrew.barton@duke.edu

Introduction

[1] Smaller phytoplankton are generally more abundant than larger cells in the ocean (Sheldon et al. 1972; Agustí et al. 1987), although many different sizes typically coexist (Cermeño et al. 2006). The mechanisms underpinning the maintenance of this size diversity remain to be fully understood. In particular, the question arises as to how larger phytoplankton are able to survive in the ocean. Larger phytoplankton are at a significant competitive disadvantage, compared with smaller cells, in several key ways: they generally have lower specific nutrient affinities (Aksnes and Egge 1991; Edwards et al. 2012), lower maximum specific growth rates (though very small phytoplankton also tend to grow slowly; Edwards et al. 2012; Kempes et al. 2012; Marañón et al. 2013), and increased self-shading of photosynthetic pigments (Duyens 1956; Finkel et al. 2004).

[2] Yet large cells persist, and even flourish, in a range of ocean habitats. One prominent hypothesis explaining their persistence is that zooplankton grazing prevents the population of smaller photoautotrophs from growing to the point of consuming all available nutrients and excluding larger, less competitive cells (Armstrong 1994; Kiørboe 2008; Ward et al. 2012).

In essence, quickly growing small grazers cap the population of small phytoplankton and liberate resources for other, larger phytoplankton. Another intriguing possibility is that chaotic dynamics within the phytoplankton community or between predators and prey may help sustain many types of phytoplankton (Huisman et al. 2006; Benincà et al. 2008; Kenitz et al. 2013). Aside from these explanations, large cells have a number of physiological advantages that may aid their survival. Their ability to store nutrients is greater than in smaller cells, and they may employ "luxury uptake" of nutrients when resources are abundant (Sunda and Huntsman 1995; Tozzi et al. 2004; Verdy et al. 2009). The same self-shading that gives larger cells lower light utilization efficiency can also protect them from photoinhibition when light levels are high (Key et al. 2010). Larger cells may also effectively regulate their buoyancy or swim rapidly to optimize growth conditions (Villareal et al. 1993; Klausmeier and Litchman 2001).

[3] Here, we examine another mechanism that may help to explain the persistence of large cells in the ocean: the effect of fine-scale turbulence on phytoplankton nutrient uptake. Energy is imparted to the ocean by wind, buoyancy forcing, and tides and is transferred from large to successively smaller eddies until it is eventually dissipated by viscosity (Tennekes and Lumley 1972). The length scale of these smallest turbulent eddies ranges from ~300 to 10,000 μm, in strongly and weakly turbulent conditions, respectively (Table 1). This ubiquitous fine-scale turbulence is believed to enhance the nutrient uptake and subsequent growth of larger phytoplankton, whereas smaller cells should be mostly unaffected (Lazier and Mann 1989; Karp-Boss et al. 1996; Guasto et al. 2012). Laboratory experiments have shown that turbulence, holding other variables equal, enhances the growth of larger cells to a greater extent than for smaller cells (e.g., Cózar and Echevarría 2005; Peters et al. 2006). However, the ecological effects of fine-scale fluid turbulence on a diverse phytoplankton community have not yet been fully evaluated. Under what levels of turbulence, and for what cell sizes, is the effect of turbulence on nutrient uptake rates likely to be important? Where and when might this mechanism play an important ecological role in the ocean?

Table 1 Characteristic values of turbulent kinetic energy dissipation rate (ε), the Kolmogorov length scale for the smallest eddy (η), and the Batchelor length scale for stirring (η_b) for differing surface ocean habitats. Adapted from Kiørboe and Saiz (1995).

Habitat	ε (m^2 s^{-3})	η (μm)	η_b (μm)
Open ocean	10^{-10} to 10^{-6}	1003–10030	25–248
Shelf seas	10^{-7} to 10^{-6}	1003–1784	25–44
Coastal zones	10^{-7} to 10^{-4}	317–1784	8–44
Tidal fronts	10^{-5}	564	14

[4] To address these questions, we developed a size-structured phytoplankton community model where phytoplankton competed for a single limiting nutrient and their functional traits were constrained by cell size (e.g., Baird and Suthers 2007; Banas 2011). We adopted an established parameterization for how nutrient uptake varies as a function of turbulence and cell size (following Karp-Boss et al. 1996; Metcalfe et al. 2004; Peters et al. 2006). This idealized trait-based model allowed us to examine the equilibrium response of the phytoplankton community to a range of turbulence and grazing conditions and to identify circumstances for which the turbulent effect on phytoplankton nutrient uptake was most and least likely to have ecological significance. We placed the model results in an environmental context by mapping the regional and seasonal variations in turbulent kinetic energy (TKE) dissipation rates and nitrate concentration in the North Atlantic Ocean. In so doing, we identified oceanographic regimes where the effect of fine-scale turbulence may play an important ecological role.

Fine-Scale Turbulence and Its Impacts on Phytoplankton

[5] The dissipation rate of TKE, ε (m^2 s^{-3}), varies rapidly in time and space by up to several orders of magnitude in response to physical forcing (Oakey 1985; MacKenzie and Leggett 1993; Skyllingstad et al. 1999). In open ocean waters, ε is generally greater at the surface and decreases with depth (MacKenzie and Leggett 1993), though observations indicate that thin layers and patches of enhanced dissipation rates may occur below the surface within the mixed layer (Gregg and Horne 2009; Smyth et al. 2013). More energetic zones, including tidal channels, fronts, storms, and breaking waves, may generate very high ε (~10^{-4} m^2 s^{-3}), while much of the surface ocean typically exhibits lower dissipation

rates on average ($\sim 10^{-7}$ m^2 s^{-3}; Oakey 1985; MacKenzie and Leggett 1993; Skyllingstad et al. 1999). Different regions of the ocean experience characteristic ranges of ε (Table 1).

[6] The scale of the smallest turbulent eddies depends on ε and occurs on approximately the Kolmogorov length scale, or η $(=(\nu^3\varepsilon^{-1})^{1/4})$, where ν is the kinematic viscosity of water (m^2 s^{-1}; see Table 2 for this and other parameter values). Greater dissipation rates are associated with smaller turbulent eddies (Table 1, Fig. 1), with $\sim$2000 μm being the scale typical of the surface ocean mixed layer (based on $\varepsilon = 10^{-7}$ m^2 s^{-3}). In comparison, the equivalent spherical diameter of diatoms varies from $\sim$2 to 200 μm, though colonies of cells such as chains and mats can be much larger. When viewed in this perspective, only the largest cells or colonies approach the size of the smallest turbulent motions (Fig. 1), which suggests that turbulence has no effect on phytoplankton nutrient uptake. However, the diffusion-limited resource concentration boundary layers enveloping phytoplankton are generally much larger than the cells themselves (Fig. 2). These concentration boundary layers are generated when nutrient uptake reduces the nutrient concentration at the cell surface below that of the bulk medium, establishing a concentration gradient maintained by diffusion, and extend outward approximately one cell radius or much more from the cell surface (Wolf-Gladrow and Riebesell 1997; Raven 1998). As fine-scale turbulent eddies and associated

Table 2 Parameter values, where allometric traits (μ_i^{max}, V_i^{max}, Q_i^{min}, and k_i) scale with cell volume.

Symbol	Parameter	Units	Value
N	Nutrient concentration	μmol N m^{-3}	
X_i	Number density	cells m^{-3}	
P_i	Biomass	μmol N m^{-3}	
Q_i	Internal quota	μmol N cell^{-1}	
μ_i	Growth rate	d^{-1}	
μ_i^{max}	Maximum growth rate	d^{-1}	$3.49\text{Vol}^{-0.15}$ [a]
V_i^{max}	Maximum uptake rate	μmol N cell^{-1} d^{-1}	$9.10 \times 10^{-9}\text{Vol}^{0.67}$ [b]
Q_i^{min}	Minimum internal quota	μmol N cell^{-1}	$1.36 \times 10^{-9}\text{Vol}^{0.77}$ [b]
k_i	Half-saturation nutrient concentration	μmol N m^{-3}	$0.17\text{Vol}^{0.27}$ [b]
k_i^T	Turbulent half-saturation nutrient concentration	μmol N m^{-3}	$k(Sh)^{-1}$
R_i^*	Minimum subsistence nutrient concentration	μmol N m^{-3}	
α	Nutrient affinity	m^3 cell^{-1} d^{-1}	$V_i^{max}(k_i^T)^{-1}$
d	Dilution rate	d^{-1}	0.1
m_z	Implicit clearance rate	m^3 cell^{-1} d^{-1}	10^{-10} to 10^{-8}
N_o	Input nutrient concentration	μmol N m^{-3}	8.0×10^3
r	Cell radius	μm	0.5–100
Sh	Sherwood number	—	
Pe	Péclet number	—	
ε	Turbulent kinetic energy dissipation rate	m^2 s^{-3}	10^{-10} to 10^{-4}
$\overline{\varepsilon_h}$	Average ε in mixed layer	m^2 s^{-3}	
ν	Kinematic viscosity of water	m^2 s^{-1}	1.004×10^{-6} [c]
D	Molecular diffusivity (phosphate)	m^2 s^{-1}	6.12×10^{-10} [c]
C_D	Drag coefficient	—	0.0015 [d]
ρ_a	Density of air at sea level	kg m^{-3}	1.2
ρ_w	Density of surface sea water	kg m^{-3}	1025
κ	Von Kármán constant	—	0.41 [e]
z	Depth	m	
h	Mixed layer depth	m	

[a] Tang (1995).
[b] Litchman et al. (2007).
[c] Metcalfe et al. (2004).
[d] Kara et al. (2007)
[e] Högström (1985).

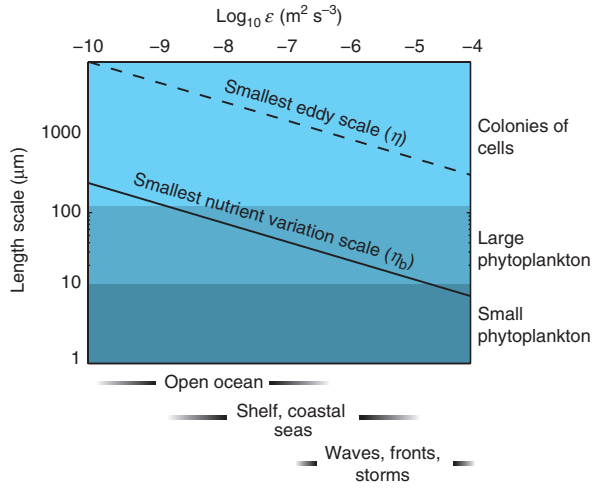

Fig. 1 Length scale for the smallest turbulent eddies (Kolmogorov scale η, µm) and smallest nutrient variations caused by stirring (Batchelor scale η_b, µm) for turbulent kinetic energy dissipation rates ($\log_{10}$ ε, m^2 s^{-3}) characteristic of a range of surface ocean habitats and conditions. As ε increases, both η $(=(\nu^3\varepsilon^{-1})^{1/4})$ and η_b $(=(\nu D^2\varepsilon^{-1})^{1/4})$ decrease in size, and successively smaller size scales are affected by turbulent fluid motion and associated heterogeneities in the nutrient field.

linear velocity shear begin to erode and distort this concentration boundary layer around larger cells, the inward diffusive flux of nutrients increases (Fig. 2; Pasciak and Gavis 1975; Lazier and Mann 1989; Karp-Boss et al. 1996). In contrast, small cells and their concentration boundary layers are much smaller than η, so the cells remain relatively unaffected by turbulence. In all cases, the direct eddy transfer of nutrients to the cell surface is minimal due to the strong viscous dissipation on this scale associated with small Reynolds numbers (Karp-Boss et al. 1996).

[7] Whereas our study focuses principally on the ecological effect of turbulent distortion of cell concentration boundary layers, variations in nutrient concentrations can also occur at length scales substantially below the Kolmogorov scale. Turbulent stirring stretches nutrient patches into thin filaments, which are then diffused (Taylor and Stocker 2012). The length scale of these stirred filaments is termed the *Batchelor scale*, or η_b $(=(\nu D^2\varepsilon^{-1})^{1/4})$, where D is the molecular diffusivity of the solute (m^2 s^{-1}). η_b is ~10–250 µm, with higher turbulence driving heterogeneities on smaller scales (Karp-Boss et al. 1996). Hence, there is significant overlap between the length scales of stirred filaments and much of the phytoplankton size spectrum (Fig. 1), and variations in these scales have the potential to affect marine ecosystems. For example, motile microbes are able swim toward nutrient-rich filaments, gaining a competitive advantage over their nonmotile competitors in environments of intermediate turbulence (Taylor and Stocker 2012).

[8] Thus, variations in the turbulent flow field (η) affect the largest cells and colonies and their concentration boundary layers at high turbulence, and

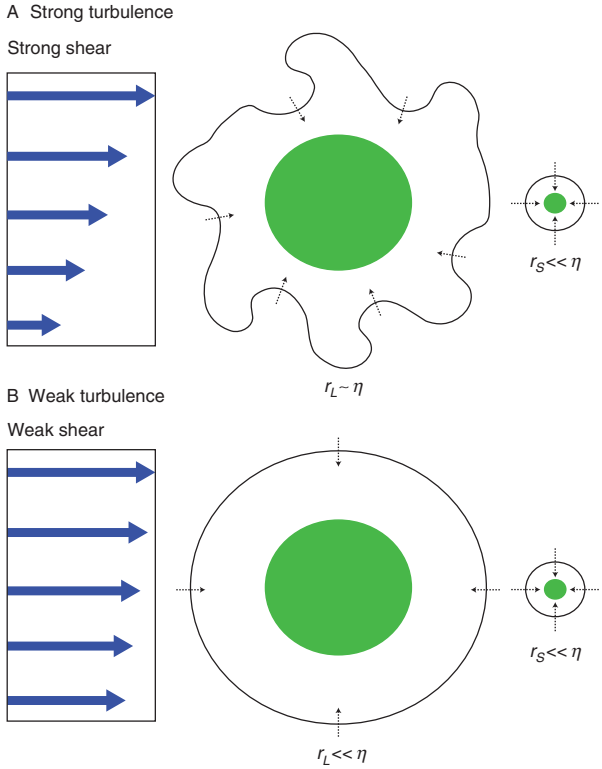

Fig. 2 Schematic of large (r_L) and small (r_S) phytoplankton cells (green circles) in strong (A) and weak (B) turbulence. A nutrient-depleted concentration boundary layer develops around the cells that has a thickness comparable to or larger than the cell radius (solid black line around the cells). Diffusion delivers nutrients from the replete background, through the depleted concentration boundary layer, to the cell surface (dashed black arrows). In strong turbulence (A), turbulent eddies have smaller horizontal scales, η, and cells experience stronger linear shear (blue arrows). Here, the horizontal scale of turbulent eddies approaches that of large phytoplankton cells and their concentration boundary layers, $r_L \sim \eta$. The concentration boundary layer around larger cells is deformed, enhancing the effective diffusive supply of nutrients, whereas the concentration boundary layer of smaller cells remains unaffected ($r_S \ll \eta$). In weak turbulence with weaker linear shear (B), both small and large cells and their concentration boundary layers are much smaller than the scale of the smallest turbulent eddy, (r_S, $r_L \ll \eta$), and uptake is unaffected by turbulence.

stirring-driven variations in the nutrient field (η_b) are comparable to a wider range of phytoplankton cell sizes. In this article we demonstrate that, while the increase in nutrient flux due to naturally occurring levels of turbulence is modest (e.g., Pasciak and Gavis 1975), this enhancement can become ecologically important when the combined effects of zooplankton grazing and turbulence are considered.

The Effect of Turbulence on Nutrient Uptake Rates

[9] Fine-scale turbulence affects the flux of nutrients toward the cell and subsequent uptake (see parameterizations by Metcalfe et al. 2004; Peters et al. 2006). Small cells are largely unaffected because they are substantially smaller than the scales of turbulent motion, whereas for larger cells uptake increases with turbulence at low resource concentrations and saturates at high resource concentrations.

[10] Nutrient uptake (V, μmol N cell^{-1} d^{-1}) in phytoplankton is typically approximated as a Michaelis–Menten saturating function of nutrient concentration (N, μmol N m^{-3}):

$$V = V^{\max}\frac{N}{N+k}, \tag{1}$$

where k (μmol N m^{-3}) is the half-saturation nutrient concentration and $V^{\max}$ (μmol N cell^{-1} d^{-1}) is the maximum possible uptake rate for a given cell (Pasciak and Gavis 1974; Armstrong 2008; Ward et al. 2011). With abundant nutrients ($N \gg k$), $V \approx V^{\max}$. $V^{\max}$ is independent of turbulence because it is determined by the physiological properties of the cell (Aksnes and Egge 1991; Aksnes and Cao 2011). Uptake in this limit is constrained by the rate of cross-membrane transport rather than the flux of nutrients toward the cell, and thus turbulence does not affect uptake.

[11] In contrast, at low N ($N \ll k$), $V \approx V^{\max}k^{-1}N$. Uptake increases linearly with N with a slope of the resource affinity, or α ($=V^{\max}k^{-1}$; m^3 cell^{-1} d^{-1}). Uptake for all but the very smallest cells is no longer limited by cross-membrane transport but instead by the flux of nutrients toward the cell. Turbulence increases this effective diffusive flux, which is parameterized by increasing affinity by a factor of *Sh*, the nondimensional Sherwood number (the ratio of the total flux to the diffusive flux; see the Appendix for further explanation; Metcalfe et al. 2004; Peters et al. 2006). In our model, we achieved this increase in nutrient affinity by calculating a modified turbulent half-saturation concentration (k^T) for each phytoplankton and level of turbulence:

$$k^T = kSh^{-1}. \tag{2}$$

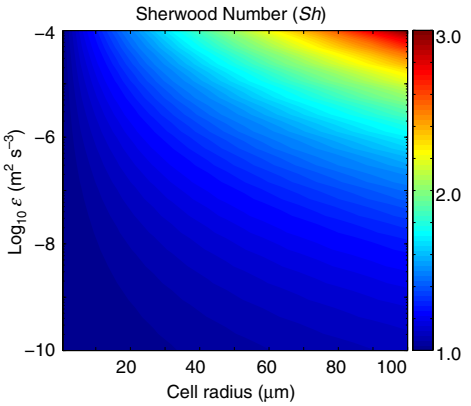

Fig. 3 Sherwood number *Sh* for a range of cell radii (μm) and turbulent dissipation rates ($\log_{10}$ ε, m^2 s^{-3}). *Sh* increases with phytoplankton cell size and turbulence but is close to 1 for small cells or in quiescent environments. *Sh* was calculated following Karp-Boss et al. (1996).

[12] We calculated *Sh* (and subsequently k^T) for a range of cell radii and ε following Karp-Boss et al. (1996), who developed formulas for *Sh* as a function of the turbulent Péclet number, *Pe*. *Pe* describes the relative importance of advective and diffusive flux of nutrients to the cell, $Pe = r^2D^{-1}(\varepsilon\nu^{-1})^{1/2}$, where r is the cell radius. For $Pe \leq 0.01$, $Sh = 1 + 0.29Pe^{1/2}$; for $Pe \geq 100$, $Sh = 0.55Pe^{1/3}$; for $0.01 < Pe < 100$, *Sh* is the mean of $1.014 + 0.150Pe^{1/2}$ and $0.955 + 0.344Pe^{1/3}$. *Pe*, and consequently *Sh*, increases with cell size and ε, thus indicating that the flux of nutrients toward the cell is enhanced by turbulent motion (Fig. 3). For example, the delivery of nutrients to the surface of a 100-μm radius cell increases by a factor of ~3 from a low- to high-turbulence environment (Fig. 3). For lower turbulence levels and smaller cell sizes, the increase in nutrient delivery is smaller, and it becomes negligible ($Sh \approx 1$) for small cells or in quiescent conditions (Karp-Boss et al. 1996; Mann and Lazier 1996). For turbulence levels characteristic of the open ocean surface (~10^{-7} m^2 s^{-3}), the increase is modest but may still be important under certain ecological conditions.

Methods

Modeling the Combined Effects of Turbulence and Grazing on Phytoplankton Communities

[13] We incorporate the parameterization for nutrient uptake (Eq. 2) into a size-structured phytoplankton community model and examine the combined ecological effects of fine-scale turbulence and zooplankton grazing for a range of turbulence and grazing regimes. The model includes i phytoplankton types (X_i, cells m^{-3}) competing for one limiting resource (N, μmol N m^{-3}) in a chemostat-like environment. In all model simulations, we use 40 phytoplankton sizes, with radii distributed uniformly in log space from 0.5 to 100 μm. The model considers spherical, nonmotile photoautotrophs, possible analogues for important marine phytoplankton groups such as cyanobacteria, picoeukaryotes, coccolithophorids, and diatoms. The model does not represent cellular motility, gravitational sinking, and other trophic strategies (e.g., Barton et al. 2013). Cell growth is a function of internal nutrient quota (Q_i, μmol N $cell^{-1}$), rather than environmental concentration (Droop 1968). Nutrient uptake (V_i, μmol N $cell^{-1}$ d^{-1}) follows Michaelis–Menten kinetics, as modified by turbulence, and the internal quota is depleted through cellular growth (μ_i, d^{-1}). Cells are lost by dilution (d, d^{-1}) and grazing (m_z, m^3 $cell^{-1}$ d^{-1}). We have adopted a quadratic loss form of implicit grazing not tied to turbulence, which is consistent with a system where the predator–prey interaction is of the Holling II form (Holling 1965), prey densities are low and limiting, and the biomasses of the grazer and phytoplankton are thus proportional. Though idealized, this form of grazing focuses losses to zooplankton grazing on the most abundant phytoplankton. The equations for cell number density for each phytoplankton size (X_i), nutrient quota (Q_i), nutrient concentration (N), and growth rate (μ_i) are

$$\frac{dX_i}{dt} = \underbrace{\mu_i X_i}_{\text{Growth}} - \underbrace{m_z X_i^2}_{\text{Implicit Grazing}} - \underbrace{dX_i}_{\text{Dilution}}, \tag{3}$$

$$\frac{dQ_i}{dt} = \underbrace{V_i^{\max}\frac{N}{N+k_i^T}}_{\text{Uptake}} - \underbrace{\mu_i Q_i}_{\text{Growth}}, \tag{4}$$

$$\frac{dN}{dt} = \underbrace{d(N_o - N)}_{\text{Nutrient Supply}} - \underbrace{\sum_i V_i^{\max}\frac{N}{N+k_i^T}X_i}_{\text{Uptake}}, \tag{5}$$

$$\mu_i = \mu_i^{\max}\left(1 - \frac{Q_i^{\min}}{Q_i}\right). \tag{6}$$

[14] The turbulent half-saturation nutrient concentration, k_i^T, depends on turbulence, such that $k_i^T = k_i(Sh_{i,\varepsilon})^{-1}$. The functional traits describing each model phytoplankton—maximum potential growth rate ($\mu_i^{\max}$, d^{-1}), minimum internal nutrient quota ($Q_i^{\min}$, μmol N $cell^{-1}$), maximum nutrient uptake rate ($V_i^{\max}$, μmol N $cell^{-1}$ d^{-1}), and half-saturation nutrient concentration (k_i, μmol N m^{-3})—scale with cell volume: $x = b\text{Vol}^a$, where allometric coefficients a and b are taken from Tang (1995) and Litchman et al. (2007), and Vol is cell volume. Nutrient input concentration (N_o, μmol N m^{-3}) is constant in the chemostat. Phytoplankton biomass (P_i, μmol N m^{-3}) is X_iQ_i. We implement the model in an idealized, well-mixed box with constant dilution rate (d) and assume that light does not limit growth. The supply of nutrients, $d(N_o - N)$, does not depend upon turbulence. We explore the system sensitivity to a range of grazing regimes by varying m_z, from relatively weak to strong top-down pressure. The values for m_z fall centrally within the range of observed zooplankton clearance rates (Kiørboe 2011), assuming a predator/prey abundance ratio of ~1:1000 (following on Agustí et al. 1987; Hansen et al. 1994). See Table 2 for model parameters.

[15] We diagnose the minimum equilibrium nutrient concentration at which growth and loss processes exactly balance for each phytoplankton type, or R_i^* (Tilman 1981; Dutkiewicz et al. 2009; Ward et al. 2011). R_i^* offers insight on the relative fitness at equilibrium of each cell size for each turbulence and grazing level and is diagnosed from Eq. 4 by setting $\frac{d}{dt} = 0$ and rearranging:

$$R_i^* = \frac{\mu_i^* Q_i^* k_i^T}{V_i^{\max} - \mu_i^* Q_i^*}. \tag{7}$$

[16] We use values of Q_i^* and μ_i^* after 100 yr of model integration (where the asterisk denotes the equilibrium value). With a single resource, cell sizes

with higher R_i^* will ultimately be excluded by those with lower R_i^*, and species with equal R_i^* can coexist in this model (Barton et al. 2010).

Estimating Turbulent Kinetic Energy Dissipation Rates in the Ocean Surface

[17] TKE in the open ocean is primarily input from the wind and is rapidly dissipated locally; only a very small part of this energy input by the wind is converted into potential energy and aids the thickening of the mixed layer (Denman 1973; Kullenberg 1976). Based on this balance between the winds and local dissipation, the vertical profile of ε can be diagnosed from observed surface wind speed by using an established closure (Denman 1973; Oakey 1985; MacKenzie and Leggett 1993):

$$\varepsilon(z) = \left(\frac{\rho_a}{\rho_w} C_D\right)^{3/2} \frac{U_{10}^3}{\kappa z}, \quad (8)$$

where U_{10} is the wind speed at 10 m above sea level, ρ_a is the density of air at sea level pressure, ρ_w is the density of surface seawater, C_D is the drag coefficient, κ is the Von Kármán constant, and z is the depth below sea level. This prediction for the ε profile from the winds (Eq. 8) agrees reasonably well with observations of ε in the surface ocean (MacKenzie and Leggett 1993), apart from in deeply convective regimes, where surface buoyancy loss becomes important in the TKE budget. By integrating ε over the mixed layer thickness, h, the average ε in the mixed layer, $\overline{\varepsilon_h}$, is obtained:

$$\overline{\varepsilon_h} = \frac{1}{h}\left[\int_{-h}^{0} \varepsilon(z) dz\right]. \quad (9)$$

[18] To calculate $\varepsilon(z)$ profiles, monthly mean surface winds (m s^{-1}) were used from National Centers for Environmental Prediction and National Center for Atmospheric Research (NCEP/NCAR) Reanalyses (Kalnay et al. 1996), where the wind speed has been calculated at 6-h intervals and then averaged over the month. $\varepsilon(z)$ was then averaged over the mean mixed layer depth, using the monthly climatology of de Boyer Montégut et al. (2004).

[19] The total input of TKE from the wind and the resulting dissipation is further decomposed into components from the time-averaged and synoptic, or eddy, wind. The total contribution of the wind to the TKE budget is proportional to $\overline{U_{10}^3}$, and the synoptic component is given by $\overline{U_{10}^3} - (\overline{U_{10}})^3$, where $(\overline{U_{10}})^3$ is

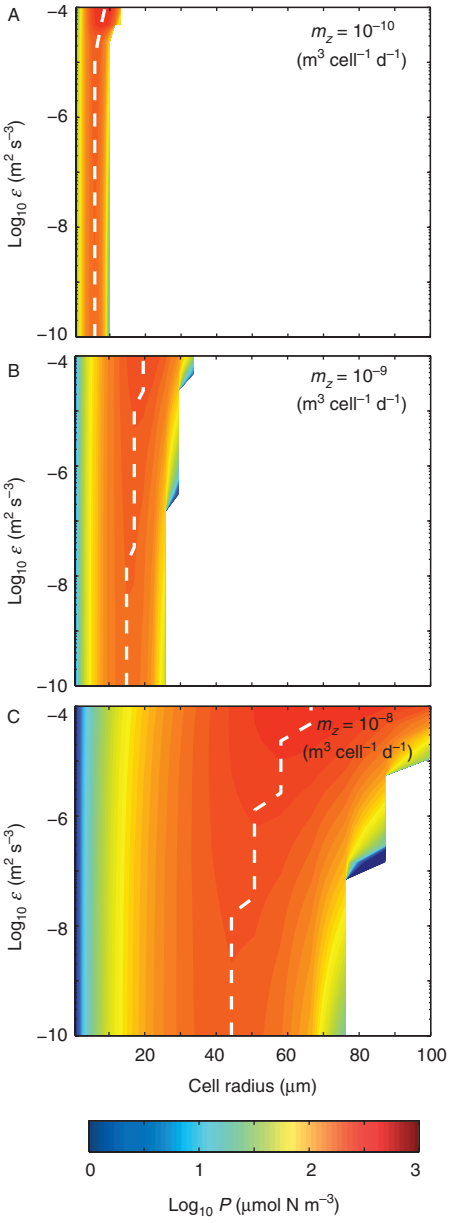

Fig. 4 Equilibrium phytoplankton biomass (Log$_{10}$ P, μmol N m^{-3}) for each size class (r, μm) and turbulence level (log$_{10}$ ε, m^2 s^{-3}) for a range of zooplankton grazing pressures (m^3 cells^{-1} d^{-1}): $m_z = 10^{-10}$ (A), $m_z = 10^{-9}$ (B), and $m_z = 10^{-8}$ (C). The phytoplankton biomass is restricted to small cell sizes at low grazing pressures but includes larger cells at higher grazing. White areas indicate competitively excluded sizes ($X_i < 1$ cell m^{-3}), and the dashed white line indicates the cell size (radius) with the highest biomass at each level of turbulence.

the cube of the time-averaged wind speed (the overbar represents a temporal averaging; see the Appendix for further details). This decomposition provides insight into the mechanisms controlling the variability in dissipation rates experienced by phytoplankton.

Results

Model Experiments

[20] When integrating the phytoplankton community model over a range of turbulence levels with relatively weak grazing pressure ($m_z = 10^{-10}$ m^3 cell^{-1} d^{-1}; Fig. 4A), only a few of the smallest size classes are sustained and coexist for a given level of turbulence. The small phytoplankton size classes have lower R^* values than larger phytoplankton for each level of turbulence (Fig. 5A), and larger cells are ultimately competitively excluded in model simulations. (Competitive exclusion is defined here as $X_i < 1$ cell m^{-3}; white areas in Fig. 4 indicate sizes that are excluded.) In this weak grazing case, the size structure in R^* originates largely from the allometric differentiation of phytoplankton traits ($Q_i^{\min}$, k_i, $V_i^{\max}$, and $\mu_i^{\max}$). For a given cell size, increasing turbulence lowers R^* (from Eq. 7, recalling that $k_i^{\mathrm{T}} = k_i(Sh_{i,\varepsilon})^{-1}$), but this effect of turbulence is small compared with gross differences in fitness between large and small cells, so the larger cells are excluded at equilibrium. In other words, this turbulence mechanism plays a negligible role in the presence of weak top-down grazing pressure on smaller phytoplankton.

[21] However, as grazing pressure on the more abundant smaller cells increases (Fig. 4B,C), additional larger size classes coexist with the smaller cell sizes. This coexistence is reflected in the greater number of size classes with equivalent R_i^* at each level of turbulence (Fig. 5B,C). The large increase in R^* with increased grazing for small cells can be understood in terms of Eq. 7, where an increasing portion of nutrients taken up by the phytoplankton population is lost to predators (the quantity $V_i^{\max} - \mu_i^* Q_i^*$ decreases). In effect, grazing in the model minimizes the competitive advantages that smaller cells have over large phytoplankton. The effect of turbulence on equilibrium ecosystem structure is also more apparent. For example, an increase in ε from 10^{-10} to 10^{-4} m^2 s^{-3} (e.g., from calm to turbulent conditions) in the presence of strong grazing pressure ($m_z = 10^{-8}$ m^3 cell^{-1} d^{-1}) enables even the largest cell sizes to coexist with smaller cells, and the radius of the dominant model phytoplankton, in terms of biomass, becomes ~20 µm larger (Fig. 4C). Increasing turbulence lowers the

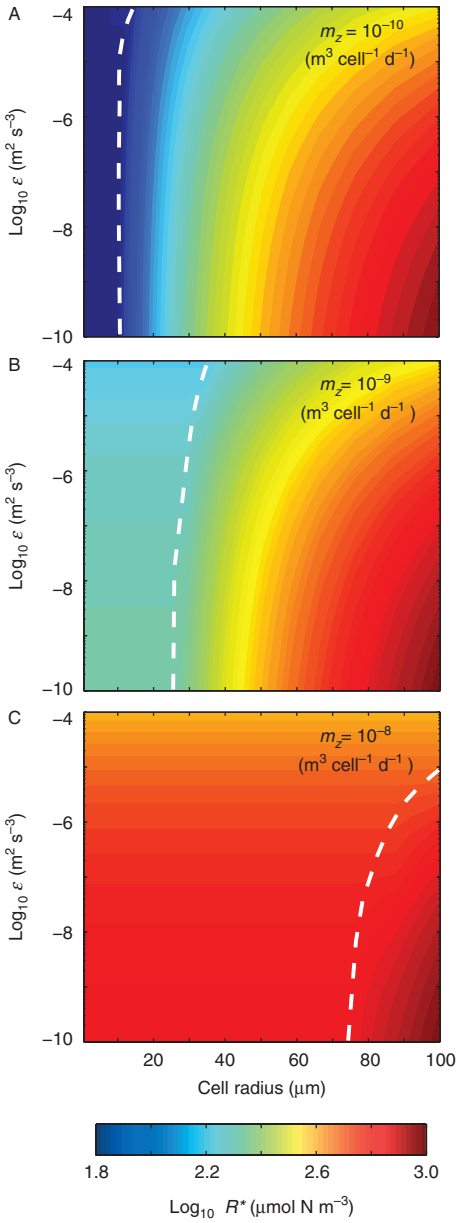

Fig. 5 Equilibrium minimum subsistence nutrient concentration, R^* (log$_{10}$ R^* µmol N m^{-3}), for each size class (r, µm) and turbulence level (log$_{10}$ ε, m^2 s^{-3}) for a range of zooplankton grazing pressures (m^3 cells^{-1} d^{-1}): $m_z = 10^{-10}$ (A), $m_z = 10^{-9}$ (B), and $m_z = 10^{-8}$ (C). Sizes to the left of the dashed white line have equal R^* and coexist, while sizes to the right have higher R^* and are competitively excluded. For a given cell size, increasing turbulent dissipation rate ε decreases R^* and so alters the equilibrium community structure.

effective R_i^* for larger cells to a greater extent than for smaller cells, because of the dependence of R_i^* on turbulent half-saturation concentration k_i^T. Thus, our model experiments suggest that turbulence may play a quantitative, ecological role in the ocean where top-down pressure is strong and turbulence is high. This strong top-down control of small phytoplankton has been observed in a range of habitats in the ocean, particularly in stratified waters, where growth of small phytoplankton is nearly balanced by zooplankton grazing (Lessard and Murrell 1998; Landry et al. 2000; Cáceres et al. 2013).

Linking Estimated Turbulent Kinetic Energy Dissipation Rates to Model Results

[22] Our model experiments suggest that for relatively high turbulent dissipation rates (qualitatively defined here as $\varepsilon \sim 10^{-7}$ m^2 s^{-3}), phytoplankton nutrient uptake and community structure begin to be affected, whereas communities are largely unaffected at low levels of turbulence. Characteristic turbulent dissipation rates experienced by phytoplankton in a well-mixed surface layer in the open ocean are presented in Fig. 6.

[23] In summer and winter, the average ε in the mixed layer is greatest in zones of intense mid-latitude westerly and lower-latitude trade winds ($\overline{\varepsilon_h} \sim 10^{-7}$ to 10^{-6} m^2 s^{-3}) and weakest within the core of the subtropical gyre ($\overline{\varepsilon_h} \sim 10^{-8}$ m^2 s^{-3}; Fig. 6A, D). TKE dissipation due to time-averaged winds is enhanced along the path of the westerly winds at mid-latitudes and the easterly trade winds at lower latitudes (Fig. 6B,E). The maxima in ε due to the time-averaged winds is less marked beneath the westerly winds at mid-latitudes due to the thicker mixed layer diluting the turbulence, compared with larger values beneath the trade winds. The eddy contribution represents the effect of daily variations in the wind, particularly including the passage of synoptic-scale weather systems. The eddy contribution is particularly dominant along the westerly wind belt at mid-latitudes (Fig. 6C,F), extending over the northern flank of the subtropical gyre and much of the subpolar gyre. Here, much of the turbulent dissipation experienced by phytoplankton is input by synoptic events rather than the time-averaged winds.

[24] These estimates of TKE dissipation rates suggest that mean levels of turbulence in the surface

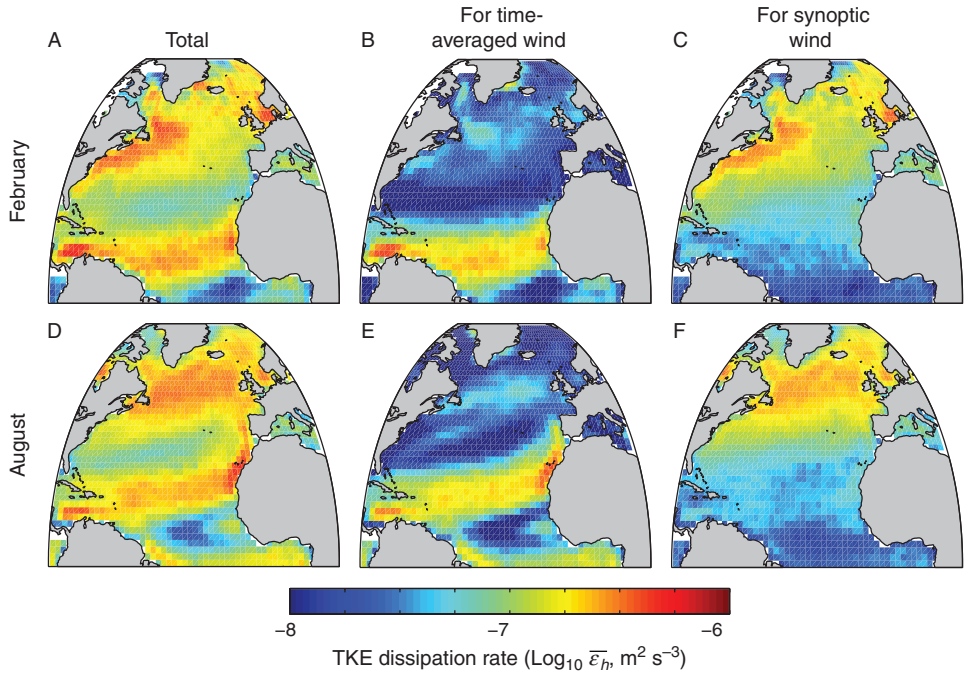

Fig. 6 Average turbulent kinetic energy dissipation rates in the mixed layer ($\log_{10}\ \overline{\varepsilon_h}$, m^2 s^{-3}) due to the total (A, D), time-averaged (B, E), and eddy, or synoptic, components (C, F) of the wind for February (A–C) and August (D–F).

ocean can approach magnitudes that affect phytoplankton community structure. This is particularly true in the North Atlantic subpolar gyre and trade wind belt, where the turbulent dissipation is driven principally by eddy and mean winds, respectively. Although these estimates indicate regions of generally low or high mean ε, observations indicate that ε is quite variable and may be much higher or lower than mean values at a given time (Skyllingstad et al. 1999; D'Asaro et al. 2011).

Discussion

[25] A wide range of phytoplankton cell sizes typically coexist in the ocean, although the mechanisms that maintain this diversity of size are not well understood. In general, smaller phytoplankton are more effective gleaners of scarce resources than larger cells, whose growth is often limited by the diffusion of nutrients toward the cell surface (Raven 1998). The results of this study indicate that the presence of large cells may be enhanced by the combined effects of grazing and turbulence. Fine-scale fluid turbulence has been shown to enhance the flux of nutrients to the cell surface, primarily by distorting the shape of the diffusive concentration boundary layer surrounding cells, and thereby increasing a cell's resource affinity. The resulting enhanced uptake is most pronounced for large cells in strong turbulence (Karp-Boss et al. 1996; Metcalfe et al. 2004; Peters et al. 2006). Hence, turbulence may provide a mechanism by which larger cells can compete with smaller cells under certain conditions.

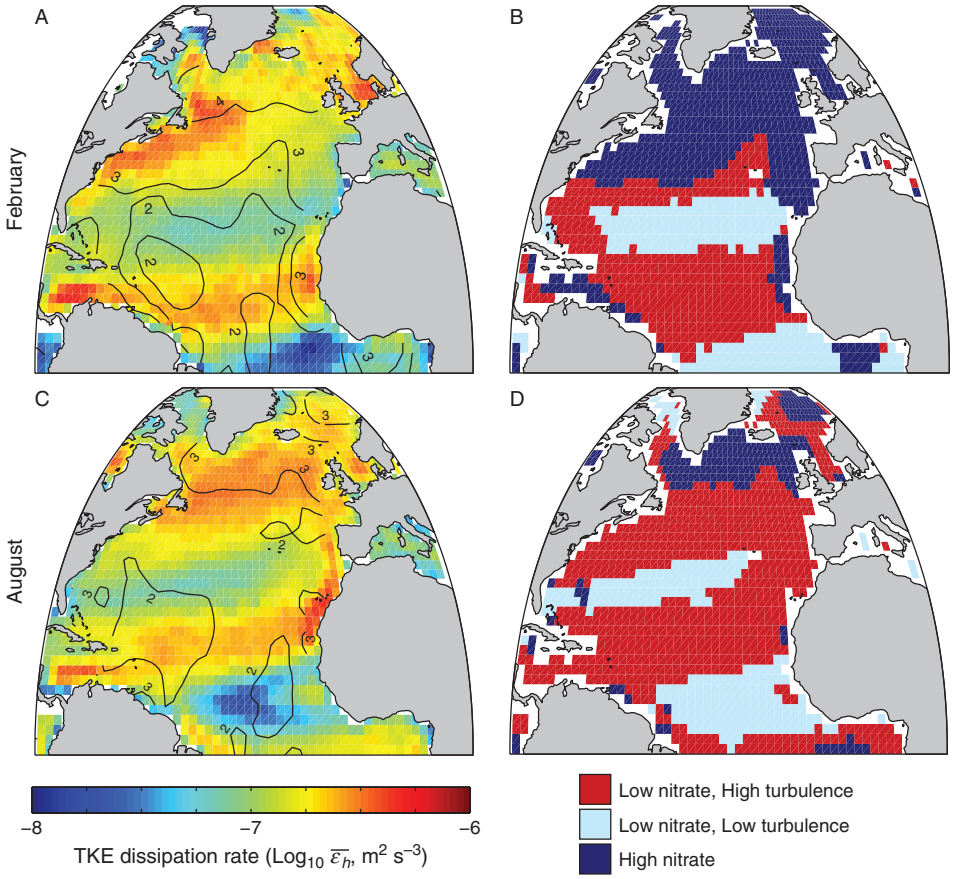

Fig. 7 Total turbulent kinetic energy dissipation rates ($\log_{10}\ \overline{\varepsilon_h}$, $m^2\ s^{-3}$) and monthly mean nitrate concentration in the North Atlantic for February (A) and August (C) (black contours shown are Log_{10} of 10^2, 10^3, and 10^4 μmol m^{-3} of nitrate). Three regions are identified for February (B) and August (D): low nitrate ($N < 10^2$ μmol m^{-3}) and high turbulence ($\overline{\varepsilon_h} > 10^{-7}\ m^2\ s^{-3}$), shown in red; low nitrate ($N < 10^2$ μmol m^{-3}) and low turbulence ($\overline{\varepsilon_h} < 10^{-7}\ m^2\ s^{-3}$), shown in light blue; high nitrate ($N > 10^2$ μmol m^{-3}), shown in dark blue. The availability of nitrate, a key macronutrient for many phytoplankton, is determined from the World Ocean Atlas 2009 (Garcia et al. 2010) and is presented in units of micromoles per cubic meter for consistency with Figs. 4 and 5.

[26] When nutrients are abundant (i.e., $N \gg k$), such as in coastal upwelling zones or during the spring bloom in subpolar seas, the direct effect of fine-scale turbulence on nutrient uptake and community structure is likely to be minimal (e.g., dark blue areas in Fig. 7B, D). The lack of sensitivity to turbulence arises because uptake in these nutrient-replete conditions is constrained by the maximum rate of cross-membrane transport (V^{max}) or maximum specific growth rate (μ^{max}), rather than the flux of nutrients toward the cell. Instead, cells exhibiting high volume-specific uptake or specific growth rates, such as small eukaryotes and diatoms (Edwards et al. 2012), have an advantage in bloom conditions. Indeed, these opportunists have been observed to dominate the beginning of phytoplankton blooms in temperate seas (Cushing 1989; Taylor et al. 1993).

[27] In contrast, when nutrients are scarce (i.e., $N \ll k$), such as in stratified subtropical and post-bloom subpolar seas, uptake for large cells can be enhanced by turbulence (Fig. 7A,C). The effect on community structure is mediated by the strength and form of grazing pressure. With weak grazing pressure, the smaller cells always outcompete larger cells because smaller phytoplankton are able to draw the ambient nutrient concentration to lower levels at which larger sizes cannot compete (Figs. 4A, 5A). The uptake benefit of fine-scale turbulence for larger cells is not enough to compensate for the gross differences in resource uptake conferred by smaller cell size. Indeed, observations (Tarran et al. 2006) and models (Dutkiewicz et al. 2009; Ward et al. 2012) have shown that smaller cells proliferate in these oligotrophic situations.

[28] However, as grazing pressure increases (Figs. 4B,C, 5B,C), the number and size range of coexisting species increase because zooplankton grazing prevents the smaller cell sizes from consuming all the available resources (Armstrong 1994; Ward et al. 2012). Because of the nonlinear dependence of mortality on prey density, the advantage gained from high affinities by smaller cells is offset by top-down grazing pressure. The importance of turbulence in regulating community structure also increases as grazing pressure increases. With increasing turbulence, the equilibrium biomass of larger cell sizes increases due to the increased nutrient supply from turbulence. The increased turbulence can also mean the difference between competitive exclusion and survival for a larger cell.

Significance to Aquatic Environments

[29] We hypothesize that fine-scale turbulence plays an ecological role in regions with relatively low nutrient levels, well-established predator populations, and relatively high TKE dissipation rates (ε) in the mixed layer (e.g., red areas in Fig. 7B,D). In these regions, where zooplankton grazing often balances or exceeds phytoplankton growth (Lessard and Murrell 1998; Landry et al. 2000; Cáceres et al. 2013), the high average dissipation rates provide an important increase in fitness for larger cells and may help explain the observed persistence of large cells in apparently unfavorable habitats (e.g., Cermeño et al. 2006). In contrast, this turbulent mechanism may be less important in regions with similarly low nutrient conditions and established predator populations but relatively low ε (e.g., light blue areas in Fig. 7B,D). Along a meridional transect through the North Atlantic at 42° W (Fig. 8), our model results and analysis of turbulence in the surface ocean suggest that the turbulent uptake mechanism affects phytoplankton community structure most strongly where the nutricline is deep, surface nutrient concentrations are low, and TKE inputs to the surface ocean are high.

[30] Although our estimates of ε reflect mean conditions in the mixed layer, ε can vary dramatically through time due to the passage of eddies, fronts, and synoptic events such as weather systems and storms (MacKenzie and Leggett 1993; Skyllingstad et al. 1999). This is particularly true in regions where wind inputs to TKE are dominated by synoptic-scale weather systems, such as in the high and mid-latitudes (Fig. 6). This temporal variability in turbulence has several potential ecological implications. First, even within oligotrophic regions with deep nutriclines and generally lower turbulence (e.g., light blue areas in Fig. 7B,D), dissipation rates may intermittently reach levels at which turbulence may play an important ecological role. Since phytoplankton growth time scales are similar to the time scales of periodically enhanced turbulence, we hypothesize that fine-scale turbulence may provide a critical, if intermittent, increase in fitness for larger cells in regions with generally low turbulence, aiding the

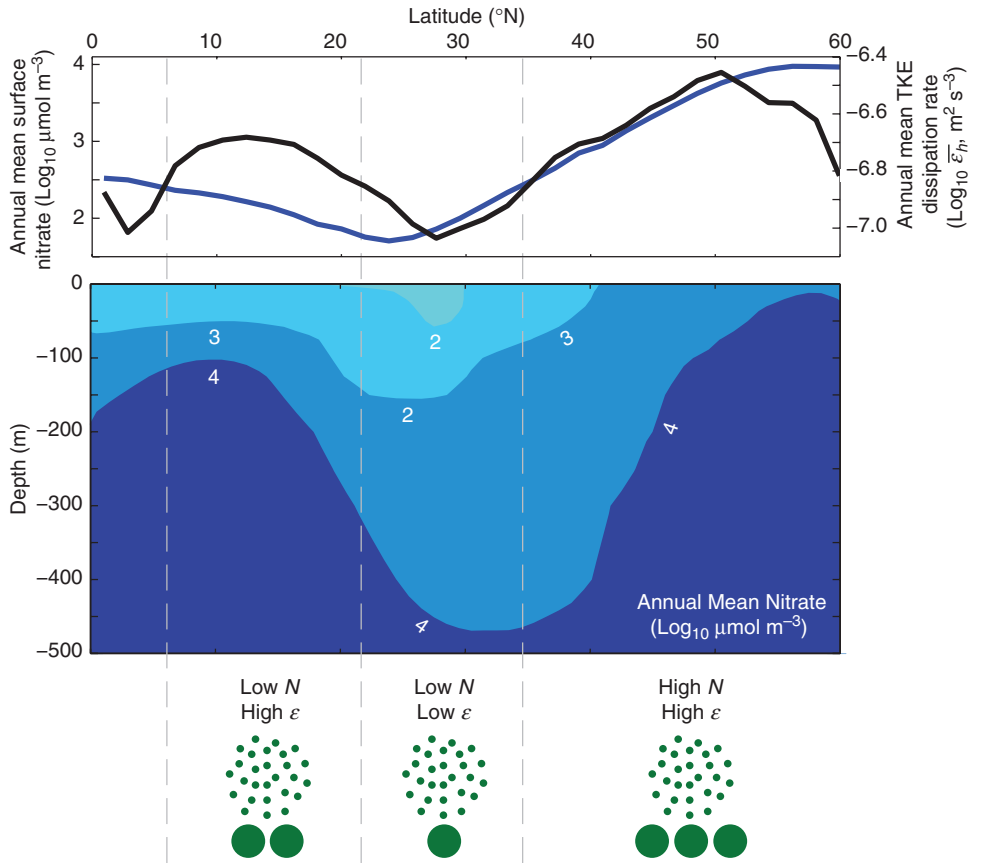

Fig. 8 Estimated annual mean turbulent kinetic energy (TKE) dissipation rates, averaged over the mixed layer ($\log_{10} \overline{\varepsilon_h}$, $m^2\ s^{-3}$; black line) and observed annual mean surface nitrate concentration ($\log_{10}$ µmol m^{-3}; blue line) along a meridional transect through the North Atlantic Ocean at 42° W. The lower panel shows the meridional depth section of observed nitrate along 42° W and indicates that the nutricline is deepest in the subtropical gyre and that it shoals somewhat near the equator and greatly in the subpolar gyre. Anticipated transitions between surface phytoplankton communities, conceptualized here by small and large green circles representing small and large cells, are indicated by the vertical, gray dashed lines. Large phytoplankton prosper in nutrient-rich regions but are also found in unfavorable, low-nutrient habitats, where we propose that high turbulence helps sustain and enhance populations of large cells. The availability of nitrate is determined from the World Ocean Atlas 2009 (Garcia et al. 2010), and ε is diagnosed as in Figs. 6 and 7.

long-term survival of a small background population of large cells. Second, within low-nutrient regions of relatively high turbulence, such as the subpolar gyre in summer, turbulent dissipation in the surface ocean is strongly tied to the passage of synoptic-scale weather systems (Fig. 6C,F). Here, the passage of storms in summer may aid the survival of larger cells, even if surface nutrient concentrations remain low. Last, observations suggest that patches or layers of higher dissipation rates may exist within the mixed layer (Gregg and Horne 2009; Smyth et al. 2013) and may provide an important, if localized and short-lived, increase in fitness for larger cells. In a broader sense, the intermittency of TKE inputs and spatial heterogeneity in dissipation rates in the surface ocean may prevent the phytoplankton community from reaching competitive equilibrium, long postulated as a means of supporting phytoplankton diversity (Hutchinson 1961).

[31] It is also interesting to speculate on whether or not this turbulent mechanism may favor formation of large colonies of cells, such as chains or mats. Though we have considered only single, spherical cells, large aggregates of cells could, depending on their geometry and behavior, benefit from increased inward nutrient flux. Colonies, however, must trade off the advantages of turbulence with the decreased nutrient uptake per cell

associated with reduced nutrient uptake area (Pahlow et al. 1997). In addition, turbulence mediates predator–prey encounter rates and zooplankton behaviors (Metcalfe et al. 2004; Kiørboe 2008; Mariani et al. 2013), which may provide a further link between turbulence and phytoplankton community structure. Although our model is most relevant to nonmotile phytoplankton, many types of phytoplankton are motile, and the ecological and biogeochemical consequences of this behavior in turbulent fluids are still being revealed (e.g., Durham et al. 2009; Taylor and Stocker 2012).

[32] We suggest that the ecological effects of turbulence on phytoplankton nutrient uptake and community structure can be evaluated and separated from other processes by combining field measurements of plankton community structure, TKE dissipation rates (ε), and resource levels (nitrogen, phosphorus, and others). Ongoing field campaigns passing through a range of turbulence and nutrient regimes, such as the Atlantic Meridional Transect program (Robinson et al. 2006), have the potential to identify transitions in phytoplankton community structure driven by turbulence and thus evaluate the hypotheses presented here (e.g., Fig. 8). Fine-scale fluid turbulence is a ubiquitous aspect of life in the surface ocean and affects the fluid microenvironments and nutrient uptake of phytoplankton in a manner dependent on their cell size. Our study suggests that fine-scale fluid turbulence has the potential to affect phytoplankton community size structure in the ocean and may help to explain how large cells are sustained within apparently unfavorable environments.

Acknowledgments ADB was supported by the U.S. National Science Foundation (NSF) International Research Fellowship Program; BAW was supported by National Aeronautics and Space Administration (NASA) and the European Community 7th Framework Programme; RGW was supported by the U.K. Natural Environment Research Council; MJF was supported by NASA and NSF. We also thank the NCEP/NCAR Reanalysis effort, the National Oceanographic Data Center, and Clément de Boyer Montégut for maintaining and providing the wind speed, nitrate, and mixed-layer depth climatologies, respectively. NCEP/NCAR Reanalysis data were provided by the National Oceanic and Atmospheric Administration's Earth System Research Laboratory, Physical Sciences Division, from their website at http://www.esrl.noaa.gov/psd/.

Appendix

Parameterization for Nutrient Uptake in Turbulent Conditions

[A1] The reduction of half-saturation concentration (k) or, alternatively, an increase in affinity (α) with increasing turbulence can be understood further by equating the rates of nutrient uptake for a cell in turbulent and still conditions. If a cell takes up all nutrients arriving at its surface immediately, then the nutrient uptake is $V = 4\pi rDN$ (Berg and Purcell 1977), where r is the cell radius and N is the ambient nutrient concentration. In the presence of turbulent motion, the enhanced uptake rate is $V^T = 4\pi rDShN$, where Sh is the nondimensional Sherwood number (Karp-Boss et al. 1996). In essence, turbulence increases the effective diffusion toward the cell. We incorporate the Sherwood number into the modified turbulent half-saturation concentration, k^T, by noting that $V^{\max}$ is equal in still and turbulent conditions and that $N = k$ when $V = \frac{1}{2}V^{max}$:

$$(4\pi rDShk^{\mathrm{T}})^{\mathrm{turb}} = \frac{V^{\max}}{2} = (4\pi rDk)^{\mathrm{still}}. \qquad \text{(A1)}$$

Rearranging Eq. A1, we see that the turbulent half-saturation nutrient concentration is

$$k^{\mathrm{T}} = kSh^{-1}. \qquad \text{(A2)}$$

Therefore, turbulence decreases k by a factor of Sh^{-1} (alternatively, α increases by a factor of Sh) and allows cells to reach uptake saturation at lower resource concentrations (Metcalfe et al. 2004; Peters et al. 2006).

Estimating Turbulent Kinetic Energy Dissipation Rates in the Surface Ocean

[A2] The input of TKE from the wind and the resulting dissipation can be decomposed into mean and eddy, or synoptic, components. For each location, the time-varying wind, $U_{10}(x,t)$, is separated into a time mean, $\overline{U_{10}(x)}$, and a time-varying eddy contribution, $U'_{10}(x,t) = U_{10}(x,t) - \overline{U_{10}}(x)$, such that $\overline{U'_{10}(x,t)} \equiv 0$. The input of TKE and resulting dissipation is proportional to the cube of the time-varying wind, using $\overline{U_{10}^3(x,t)}$ in Eq. 8, which is estimated over each month by summing the contributions from 6-h values (Fig. 6A,D).

[A3] To estimate the contribution from the time mean wind, the input of TKE and resulting dissipation are instead estimated using $(\overline{U_{10}(x)})^3$ in Eq. 8. We calculate the time mean wind, $\overline{U_{10}(x)}$, by averaging NCEP/NCAR meridional and zonal wind vectors $(\mathbf{u}, \mathbf{v})$ over the month and then calculating a monthly average wind speed, $\overline{U_{10}(x)} = (\overline{\mathbf{u}}^2 + \overline{\mathbf{v}}^2)^{1/2}$. The eddy contribution to the input of TKE and resulting dissipation is then based on the estimate using the time-varying wind minus the estimate using the time mean wind, $\overline{U_{10}^3(x,t)} - (\overline{U_{10}(x)})^3$.

References

Agustí, S., C. M. Duarte, and J. Kalff. 1987. Algal cell size and the maximum density and biomass of phytoplankton. Limnol. Oceanogr. **32**: 983–986. doi:10.4319/lo.1987.32.4.0983.

Aksnes, D. L., and F. J. Cao. 2011. Inherent and apparent traits in microbial nutrient uptake. Mar. Ecol. Prog. Ser. **440**: 41–51. doi:10.3354/meps09355.

Aksnes, D. L., and J. K. Egge. 1991. A theoretical model for nutrient uptake in phytoplankton. Mar. Ecol. Prog. Ser. **70**: 65–72. doi:10.3354/meps070065.

Armstrong, R. A. 1994. Grazing limitation and nutrient limitation in marine ecosystems—steady-state solutions of an ecosystem model with multiple food-chains. Limnol. Oceanogr. **39**: 597–608. doi:10.4319/lo.1994.39.3.0597.

Armstrong, R. A. 2008. Nutrient uptake rate as a function of cell size and surface transporter density: A Michaelis-like approximation to the model of Pasciak and Gavis. Deep Sea Res. Part I Oceanogr. Res. Pap. **55**: 1311–1317. doi:10.1016/j.dsr.2008.05.004.

Baird, M. E., and I. M. Suthers. 2007. A size-resolved pelagic ecosystem model. Ecol. Modell. **203**: 185–203. doi:10.1016/j.ecolmodel.2006.11.025.

Banas, N. S. 2011. Adding complex trophic interactions to a size-spectral plankton model: Emergent diversity patterns and limits on predictability. Ecol. Modell. **222**: 2663–2675. doi:10.1016/j.ecolmodel.2011.05.018.

Barton, A. D., S. Dutkiewicz, G. Flierl, J. Bragg, and M. J. Follows. 2010. Patterns of diversity in marine phytoplankton. Science **327**: 1509–1511. doi:10.1126/science.1184961.

Barton, A. D., Z. V. Finkel, B. A. Ward, D. G. Johns, and M. J. Follows. 2013. On the roles of cell size and trophic strategy in North Atlantic diatom and dinoflagellate communities. Limnol. Oceanogr. **58**: 254–266. doi:10.4319/lo.2013.58.1.0254.

Benincà, E., J. Huisman, R. Heerkloss, K. D. Johnk, P. Branco, E. H. Van Nes, M. Scheffer, and S. P. Ellner. 2008. Chaos in a long-term experiment with a plankton community. Nature **451**: 822–825. doi:10.1038/nature06512.

Berg, H. C., and E. M. Purcell. 1977. Physics of chemoreception. Biophys. J. **20**: 193–219. doi:10.1016/S0006-3495(77)85544-6.

Cáceres, C., F. G. Taboada, J. Höfer, and R. Anadón. 2013. Phytoplankton growth and microzooplankton grazing in the subtropical northeast Atlantic. PLoS ONE **8**: e69159. doi:10.1371/journal.pone.0069159.

Cermeño, P., E. Marañón, D. Harbour, and R. P. Harris. 2006. Invariant scaling of phytoplankton abundance and cell size in contrasting marine environments. Ecol. Lett. **9**: 1210–1215. doi:10.1111/j.1461-0248.2006.00973.x.

Cózar, A., and F. Echevarría 2005. Size structure of the planktonic community in microcosms with different levels of turbulence. Sci. Mar. **69**: 187–197.

Cushing, D. 1989. A difference in structure between ecosystems in strongly stratified waters and in those that are weakly stratified. J. Plankton Res. **11**: 1–13. doi:10.1093/plankt/11.1.1.

D'Asaro, E., C. Lee, L. Rainville, R. Harcourt, and L. Thomas. 2011. Enhanced turbulence and energy dissipation at ocean fronts. Science **332**: 318–322. doi:10.1126/science.1201515.

de Boyer Montégut, C., G. Madec, A. S. Fischer, A. Lazar, and D. Iudicone. 2004. Mixed layer depth over the global ocean: An examination of profile data and a profile-based climatology. J. Geophys. Res. **109**(C12): C12003. doi:10.1029/2004JC002378.

Denman, K. 1973. A time-dependent model of the upper ocean. J. Phys. Oceanogr. **3**: 173–184. doi:10.1175/1520-0485(1973)003<0173:ATDMOT>2.0.CO;2.

Droop, M. 1968. Vitamin B12 and marine ecology. IV. The kinetics of uptake, growth and inhibition in Monochrysis lutheri. J. Mar. Biol. Assoc. U. K. **48**: 689–733. doi:10.1017/S0025315400019238.

Durham, W. M., J. O. Kessler, and R. Stocker. 2009. Disruption of vertical motility by shear triggers formation of thin phytoplankton layers. Science **323**: 1067–1070. doi:10.1126/science.1167334.

Dutkiewicz, S., M. J. Follows, and J. G. Bragg. 2009. Modeling the coupling of ocean ecology and biogeochemistry. Global Biogeochem. Cycles **23**: GB4017. doi:10.1029/2008GB003405.

Duyens, L. N. M. 1956. The flattening of the absorption spectrum of suspensions, as compared to that of solutions. Biochim. Biophys. Acta **19**: 1–12. doi:10.1016/0006-3002(56)90380-8.

Edwards, K. F., M. K. Thomas, C. A. Klausmeier, and E. Litchman. 2012. Allometric scaling and taxonomic variation in nutrient utilization traits and maximum growth rate of phytoplankton. Limnol. Oceanogr. **57**: 554–566. doi:10.4319/lo.2012.57.2.0554.

Finkel, Z. V., A. Irwin, and O. Schofield. 2004. Resource limitation alters the 3/4 size scaling of metabolic rates in phytoplankton. Mar. Ecol. Prog. Ser. **273**: 269–279. doi:10.3354/meps273269.

Garcia, H., R. Locarnini, T. Boyer, J. Antonov, M. Zweng, O. Baranova, and D. Johnson. 2010. Nutrients (Phosphate, Nitrate, Silicate). Vol. 4 in S. Levitus [ed.], World Ocean

Atlas 2009. NOAA Atlas NESDIS 71. US Government Printing Office.

Gregg, M. C., and J. K. Horne. 2009. Turbulence, acoustic backscatter, and pelagic nekton in Monterey Bay. J. Phys. Oceanogr. **39**: 1097–1114. doi:10.1175/2008JPO4033.1.

Guasto, J. S., R. Rusconi, and R. Stocker. 2012. Fluid mechanics of planktonic microorganisms. Annu. Rev. Fluid Mech. **44**: 373–400. doi:10.1146/annurev-fluid-120710-101156.

Hansen, B., P. Bjørnsen, and P. J. Hansen. 1994. The size ratio between planktonic predators and their prey. Limnol. Oceanogr. **39**: 395–403. doi:10.4319/lo.1994.39.2.0395.

Högström, U. 1985. Von Kármán's constant in atmospheric boundary layer flow: Reevaluated. J. Atmos. Sci. **42**: 263–270. doi:10.1175/1520-0469(1985)042<0263:VKCIAB>2.0.CO;2.

Holling, C. 1965. The functional response of predators to prey density and its role in mimicry and population regulation. Mem. Entomol. Soc. Can. **97**(Suppl. S45): 5–60. doi:10.4039/entm9745fv.

Huisman, J., N. N. Pham Thi, D. M. Karl, and B. Sommeijer. 2006. Reduced mixing generates oscillations and chaos in the oceanic deep chlorophyll maximum. Nature **439**: 322–325. doi:10.1038/nature04245.

Hutchinson, G. 1961. The paradox of the plankton. Am. Nat. **95**: 137–145. doi:10.1086/282171.

Kalnay, E., et al. 1996. The NCEP/NCAR 40-year reanalysis project. Bull. Am. Meteorol. Soc. **77**: 437–471. doi:10.1175/1520-0477(1996)077<0437:TNYRP>2.0.CO;2.

Kara, A. B., A. J. Wallcraft, E. J. Metzger, H. E. Hurlburt, and C. W. Fairall. 2007. Wind stress drag coefficient over the global ocean. J. Clim. **20**: 5856–5864. doi:10.1175/2007JCLI1825.1.

Karp-Boss, L., E. Boss, and P. Jumars. 1996. Nutrient fluxes to planktonic osmotrophs in the presence of fluid motion. Oceanogr. Mar. Biol. Annu. Rev. **34**: 71–107.

Kempes, C. P., S. Dutkiewicz, and M. J. Follows. 2012. Growth, metabolic partitioning, and the size of microorganisms. Proc. Natl. Acad. Sci. USA **109**: 495–500. doi:10.1073/pnas.1115585109.

Kenitz, K., R. G. Williams, J. Sharples, O. Selsil, and V. N. Biktashev. 2013. The paradox of the plankton: Species competition and nutrient feedback sustain phytoplankton diversity. Mar. Ecol. Prog. Ser. **490**: 107–119. doi:10.3354/meps10452.

Key, T., A. McCarthy, D. A. Campbell, C. Six, S. Roy, and Z. V. Finkel. 2010. Cell size trade-offs govern light exploitation strategies in marine phytoplankton. Environ. Microbiol. **12**: 95–104. doi:10.1111/j.1462-2920.2009.02046.x.

Kiørboe, T. 2008. A Mechanistic Approach to Plankton Ecology. Princeton University Press.

Kiørboe, T. 2011. How zooplankton feed: Mechanisms, traits and trade-offs. Biol. Rev. Camb. Philos. Soc. **86**: 311–339. doi:10.1111/j.1469-185X.2010.00148.x.

Kiørboe, T., and E. Saiz. 1995. Planktivorous feeding in calm and turbulent environments, with emphasis on copepods. Mar. Ecol. Prog. Ser. **122**: 135–145. doi:10.3354/meps122135.

Klausmeier, C. A., and E. Litchman. 2001. Algal games: The vertical distribution of phytoplankton in poorly mixed water columns. Limnol. Oceanogr. **46**: 1998–2007. doi:10.4319/lo.2001.46.8.1998.

Kullenberg, G. E. B. 1976. On vertical mixing and the energy transfer from the wind to the water. Tellus **28**: 159–165. doi:10.1111/j.2153-3490.1976.tb00663.x.

Landry, M. R., J. Constantinou, M. Latasa, S. Brown, R. R. Bidigare, and M. Ondrusek. 2000. Biological response to iron fertilization in the eastern equatorial Pacific (IronEx II). III. Dynamics of phytoplankton growth and microzooplankton grazing. Mar. Ecol. Prog. Ser. **201**: 57–72. doi:10.3354/meps201057.

Lazier, J. R. N., and K. H. Mann. 1989. Turbulence and the diffusive layers around small organisms. Deep-Sea Res. **36**: 1721–1733. doi:10.1016/0198-0149(89)90068-X.

Lessard, E. J., and M. C. Murrell. 1998. Microzooplankton herbivory and phytoplankton growth in the northwestern Sargasso Sea. Aquat. Microb. Ecol. **16**: 173–188. doi:10.3354/ame016173.

Litchman, E., C. A. Klausmeier, O. M. Schofield, and P. G. Falkowski. 2007. The role of functional traits and trade-offs in structuring phytoplankton communities: Scaling from cellular to ecosystem level. Ecol. Lett. **10**: 1170–1181. doi:10.1111/j.1461-0248.2007.01117.x.

MacKenzie, B. R., and W. C. Leggett. 1993. Wind-based models for estimating the dissipation rates of turbulent energy in aquatic environments: Empirical comparisons. Mar. Ecol. Prog. Ser. **94**: 207–216. doi:10.3354/meps094207.

Mann, K. H., and J. R. N. Lazier. 1996. Dynamics of Marine Ecosystems: Biological-Physical Interactions in the Oceans. Blackwell.

Marañón, E., P. Cermeño, D. C. López-Sandoval, T. Rodriguez-Ramos, C. Sobrino, M. Huete-Ortega, J. M. Blanco, and J. Rodríguez. 2013. Unimodal size scaling of phytoplankton growth and the size dependence of nutrient uptake and use. Ecol. Lett. **16**: 371–379. doi:10.1111/ele.12052.

Mariani, P., K. Andersen, A. W. Visser, A. D. Barton, and T. Kiørboe. 2013. Control of plankton seasonal succession by adaptive grazing. Limnol. Oceanogr. **58**: 173–184. doi:10.4319/lo.2013.58.1.0173.

Metcalfe, A. M., T. J. Pedley, and T. F. Thingstad. 2004. Incorporating turbulence into a plankton foodweb model. J. Mar. Syst. **49**: 105–122. doi:10.1016/j.jmarsys.2003.07.003.

Oakey, N. 1985. Statistics of mixing parameters in the upper ocean during JASIN Phase 2. J. Phys. Oceanogr. **15**: 1662–1675. doi:10.1175/1520-0485(1985)015<1662:SOMPIT>2.0.CO;2.

Pahlow, M., U. Riebesell, and D. Wolf-Gladrow. 1997. Impact of cell shape and chain formation on nutrient acquisition by marine

diatoms. Limnol. Oceanogr. **42**: 1660–1672. doi:10.4319/lo.1997.42.8.1660.

Pasciak, W. J., and J. Gavis. 1974. Transport limitation of nutrient uptake in phytoplankton. Limnol. Oceanogr. **19**: 881–888. doi:10.4319/lo.1974.19.6.0881.

Pasciak, W. J., and J. Gavis. 1975. Transport limited nutrient uptake rates in *Ditylum brightwellii*. Limnol. Oceanogr. **20**: 604–617. doi:10.4319/lo.1975.20.4.0604.

Peters, F., L. Arin, C. Marrasé, E. Berdalet, and M. M. Sala. 2006. Effects of small-scale turbulence on the growth of two diatoms of different size in a phosphorus-limited medium. J. Mar. Syst. **61**: 134–148. doi:10.1016/j.jmarsys.2005.11.012.

Raven, J. A. 1998. The twelfth Tansley Lecture. Small is beautiful: The picophytoplankton. Funct. Ecol. **12**: 503–513. doi:10.1046/j.1365-2435.1998.00233.x.

Robinson, C., et al. 2006. The Atlantic Meridional Transect (AMT) programme: A contextual view 1995–2005. Deep Sea Res. Part II Top. Stud. Oceanogr. **53**: 1485–1515. doi:10.1016/j.dsr2.2006.05.015.

Sheldon, R., A. Prakash, and W. Sutcliffe. 1972. The size distribution of particles in the ocean. Limnol. Oceanogr. **17**: 327–340. doi:10.4319/lo.1972.17.3.0327.

Skyllingstad, E., W. Smyth, J. Moum, and H. Wijesekera. 1999. Upper-ocean turbulence during a westerly wind burst: A comparison of large-eddy simulation results and microstructure measurements. J. Phys. Oceanogr. **29**: 5–28. doi:10.1175/1520-0485(1999)029<0005:UOTDAW>2.0.CO;2.

Smyth, W. D., J. N. Moum, L. Li, and S. A. Thorpe. 2013. Diurnal shear instability, the descent of the surface shear layer, and the deep cycle of equatorial turbulence. J. Phys. Oceanogr. **43**: 2432–2455. doi:10.1175/JPO-D-13-089.1.

Sunda, W. G., and S. A. Huntsman. 1995. Iron uptake and growth limitation in oceanic and coastal phytoplankton. Mar. Chem. **50**: 189–206. doi:10.1016/0304-4203(95)00035-P.

Tang, E. 1995. The allometry of algal growth rates. J. Plankton Res. **17**: 1325–1335. doi:10.1093/plankt/17.6.1325.

Tarran, G. A., J. L. Heywood, and M. V. Zubkov. 2006. Latitudinal changes in the standing stocks of nano- and picoeukaryotic phytoplankton in the Atlantic Ocean. Deep Sea Res. Part II Top. Stud. Oceanogr. **53**: 1516–1529. doi:10.1016/j.dsr2.2006.05.004.

Taylor, A., D. Harbour, R. Harris, P. Burkill, and E. Edwards. 1993. Seasonal succession in the pelagic ecosystem of the North Atlantic and the utilization of nitrogen. J. Plankton Res. **15**: 875–891. doi:10.1093/plankt/15.8.875.

Taylor, J. R., and R. Stocker. 2012. Trade-offs of chemotactic foraging in turbulent water. Science **338**: 675–679. doi:10.1126/science.1219417.

Tennekes, H., and J. L. Lumley. 1972. A First Course in Turbulence. MIT Press.

Tilman, D. 1981. Tests of resource competition theory using four species of Lake Michigan algae. Ecology **62**: 802–815. doi:10.2307/1937747.

Tozzi, S., O. Schofield, and P. Falkowski. 2004. Historical climate change and ocean turbulence as selective agents for two key phytoplankton functional groups. Mar. Ecol. Prog. Ser. **274**: 123–132. doi:10.3354/meps274123.

Verdy, A., M. Follows, and G. Flierl. 2009. Optimal phytoplankton cell size in an allometric model. Mar. Ecol. Prog. Ser. **379**: 1–12. doi:10.3354/meps07909.

Villareal, T. A., M. Altabet, and K. Culver-Rymsza. 1993. Nitrogen transport by vertically migrating diatom mats in the North Pacific Ocean. Nature **363**: 709–712. doi:10.1038/363709a0.

Ward, B. A., S. Dutkiewicz, A. D. Barton, and M. J. Follows. 2011. Biophysical aspects of resource acquisition and competition in algal mixotrophs. Am. Nat. **178**: 98–112. doi:10.1086/660284.

Ward, B. A., S. Dutkiewicz, O. Jahn, and M. J. Follows. 2012. A size-structured food-web model for the global ocean. Limnol. Oceanogr. **57**: 1877–1891. doi:10.4319/lo.2012.57.6.1877.

Wolf-Gladrow, D., and U. Riebesell. 1997. Diffusion and reactions in the vicinity of plankton: A refined model for inorganic carbon transport. Mar. Chem. **59**: 17–34. doi:10.1016/S0304-4203(97)00069-8.

Received: 19 September 2013
Amended: 11 December 2013
Accepted: 27 December 2013